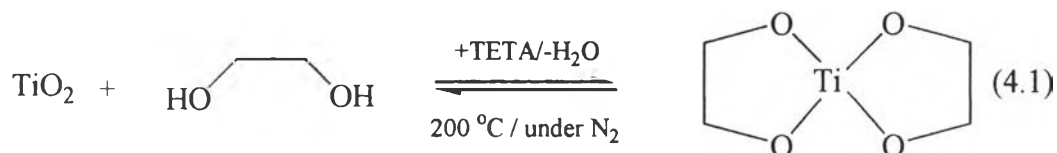


CHAPTER IV RESULTS AND DISCUSSION

4.1 Synthesis of Glycolato Titanium Precursor

Glycolato titanium precursor was synthesized via the “Oxide One Pot Synthesis” (OOPS) process using inexpensive and widely available TiO_2 as starting material, ethylene glycol and triethylenetetramine, TETA, as a base. Since water is a by-product of the reaction, it must be removed from the system to push the reaction forward, as illustrated in equation 4.1.



In this synthesis, the obtained product is in white color and exhibits outstanding high stability not only in alcohol but also in water (Wang *et al.*, 1999).

4.2 Characterization

4.2.1 Characterization of Glycolato Titanium Precursor

The synthesized and purified precursor was identified using TGA, EA, NMR, FAB⁺MS, FT-IR, SEM and XRD, as described following.

4.2.1.1 *Thermogravimetric Analysis (TGA)*

The TGA analyses of glycolato titanium were carried out in nitrogen atmosphere and the result is shown in Figure 4.1. The first weight loss around 310°-350 °C corresponds to organic ligand decomposition. The second weight loss around 360°-500 °C results from oxidation decomposition of remaining organic residue. The final ceramic yield is 46.95 %, as compared to 47.56 % for the theoretical ceramic yield based on a final ceramic product TiO_2 .

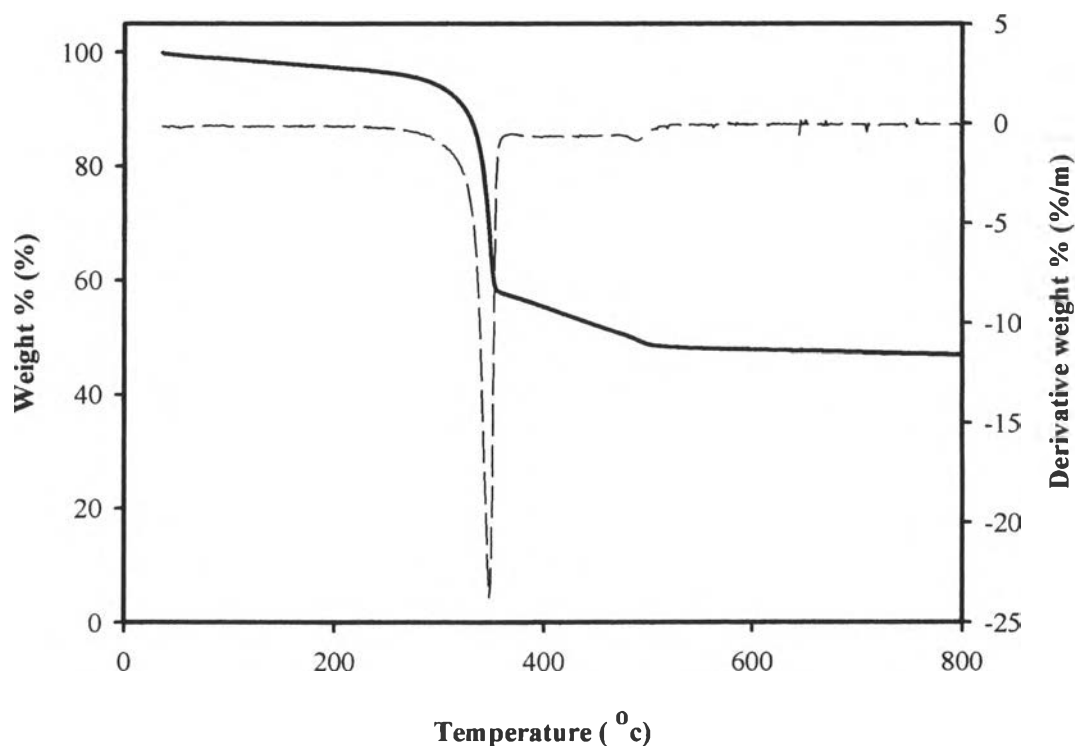


Figure 4.1 TGA profile of glycolato titanium.

4.2.1.2 Nuclear Magnetic Resonance Spectroscopy (NMR)

The solid state ^{13}C -NMR spectrum, as shown in Figure 4.2, was used to confirm the structure of glycolato titanium. The ^{13}C -NMR spectrum shows peaks at 75.9 and 79.8 ppm which can be attributed to two glycolate ligand of glycolato titanium. The reason that the spectrum splits into two peaks is two chelate ligands have different environment due to the difference in bond lengths (Wang *et al.*, 1999). The small peak at 63.8 ppm belongs to the carbon atom of free ethylene glycol.

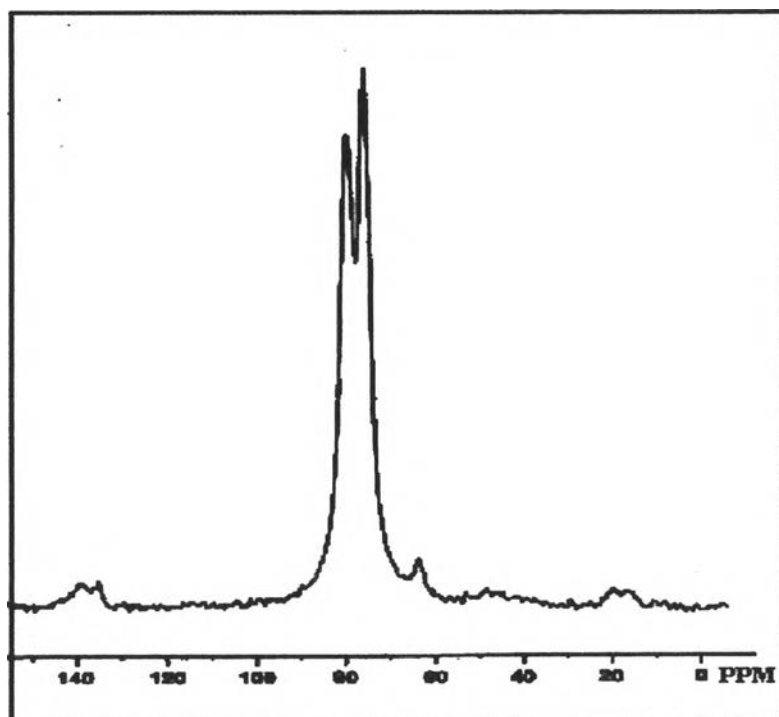


Figure 4.2 ^{13}C -NMR spectrum of glycolato titanium.

4.2.1.3 Elemental Analysis (EA)

The percent element results are shown in Table 4.1. The experimental carbon and hydrogen percentages are 27.9 % and 5.6 %, respectively, which are close to theoretical results. That means that the synthesized precursor is the expected glycolato titanium.

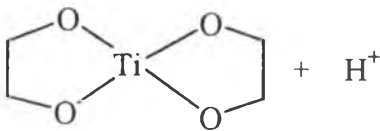
Table 4.1 Percent elements of glycolato titanium

% elements		
Results	%C	%H
experimental	27.9	5.6
theoretical	28.6	4.8

4.2.1.4 FAB⁺-MS Spectroscopy (MS)

Mass spectral analysis of glycolato titanium shows the peak at m/e 169, 8.5 % intensity, indicating the molecular ion of glycolato titanium which is easily broken to the peak at m/e 93 that is belong to ethoxy titanium. The fragment peaks at m/e 45 and 28 correspond to the ethoxy group and ethylene, respectively. The intensities of all proposed structures are shown in table 4.2.

Table 4.2 The proposed structure and the pattern of fragmentation of glycolato titanium

m/e	% Intensity	Proposed Structure
169	8.5	 + H ⁺
93	100	Ti-OCH ₂ CH ₂ + H ⁺
45	13	CH ₂ CH ₂ O + H ⁺
28	4	CH ₂ CH ₂ [•]

4.2.1.5 Fourier Transform Infrared Spectroscopy (FTIR)

IR spectrum and assignment of glycolato titanium are shown in Figure 4.3 and Table 4.3, respectively. The band around 2855-2927 cm^{-1} is assigned to the C-H stretching of glycolate ligand. Three bands at 1130, 1080 and 1042 cm^{-1} can be assigned to C-O-Ti, characteristic of glycolate ligand linked to titanium. The presence of band at 619 cm^{-1} is assigned to Ti-O stretching (Wang *et al.*, 1999).

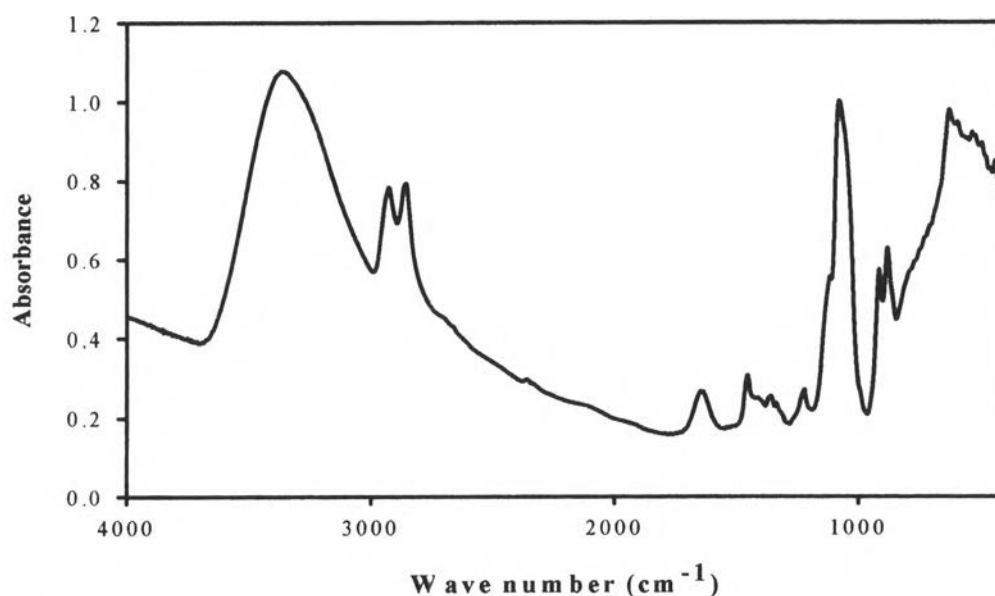


Figure 4.3 IR spectrum of glycolato titanium.

Table 4.3 Assignment of IR spectrum of glycolato titanium

Peak Positions (cm^{-1})	Assignments
3000-3500	O-H stretching (from ethylene glycol)
2855-2927	C-H stretching
1430-1450	C-H bending
1040-1130	C-O-Ti
610-650	Ti-O stretching

4.2.1.6 X-Ray Diffraction (XRD)

The XRD patterns of calcined and uncalcined glycolato titanium are shown in Figure 4.4. At room temperature, glycolato titanium has a crystal structure. At lower temperature (below 300 °C), the resulting product is amorphous, while calcining at higher temperature, a broader anatase appeared. With the increasing of the calcination temperature, the intensity of the anatase peaks became stronger and well-resolved around 900 °C, indicating that larger size particles are formed. When the calcination temperature continues increasing, small rutile peaks are coexisted with the anatase and a single phase of rutile is obtained at 1100 °C. As compared with the transformation temperature between commercial titanium alkoxides, such as tetrapropylorthotitanate (Zhang *et al.*, 2002) and synthesized product, the higher evolution of anatase-to-rutile of the synthesized product and the end of phase transition of anatase-to-rutile are terminated at higher temperatures. That means the synthesized product is suitable for preparation of high thermal stability anatase titania powder.

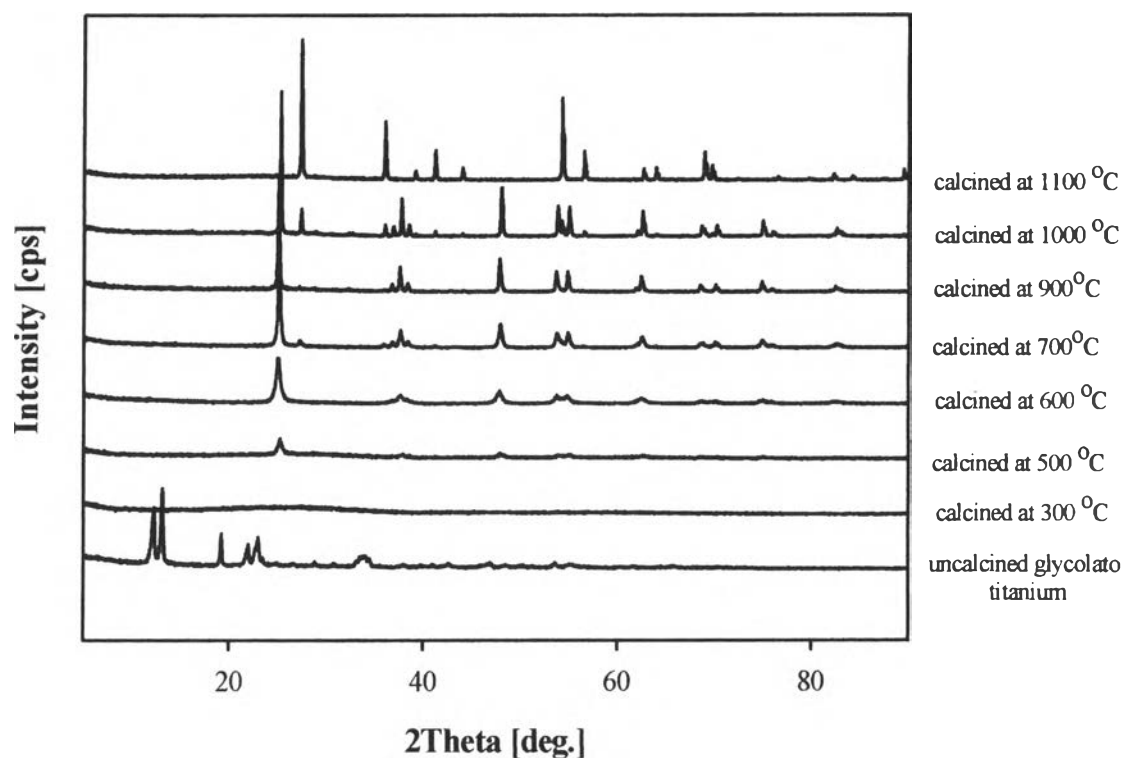
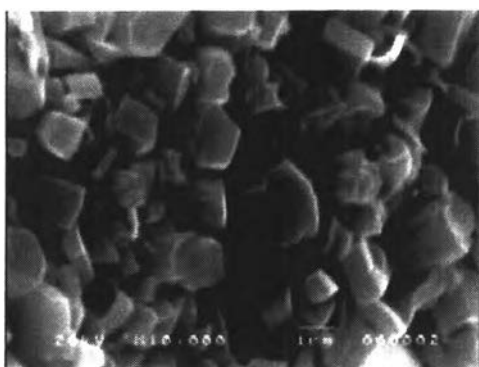


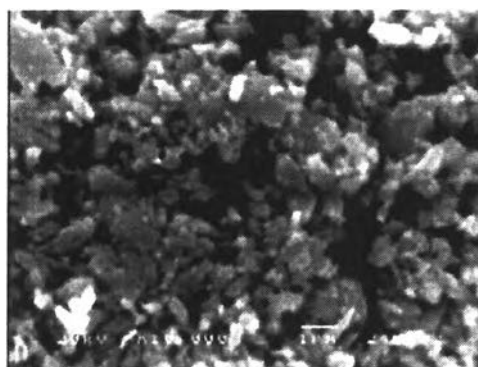
Figure 4.4 XRD patterns of glycolato titanium calcined at different temperatures.

4.2.1.7 Scanning Electron Microscopy (SEM)

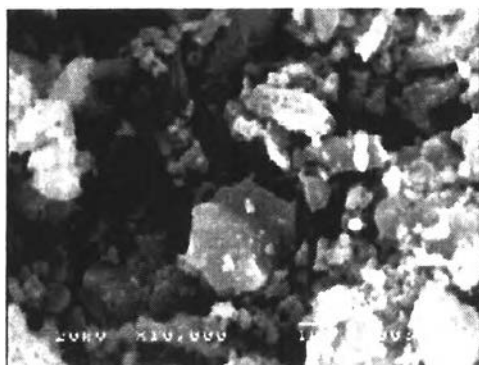
The morphology of glycolato titanium was observed by scanning electron microscopy, as shown in Figures 4.5a-f. Uncalcined glycolato titanium, as shown in Figure 4.5a, has a needle-like crystal structure (Wang *et al.*, 1999 and supported by the XRD results in Figure 4.4). At 300 °C glycolato titanium shows amorphous, as shown in Figure 4.5b. With the increasing of calcination temperatures (500° to 900 °C), the anatase crystal titania starts to form and the particle size increases with increasing temperature due to the agglomeration, as shown in Figures 4.5c-e. The rutile crystal titania can be observed at 1100 °C. As compared between the crystal structure, anatase crystal (Figures 4.5c-e) has more porous than the rutile (Figure 4.5f).



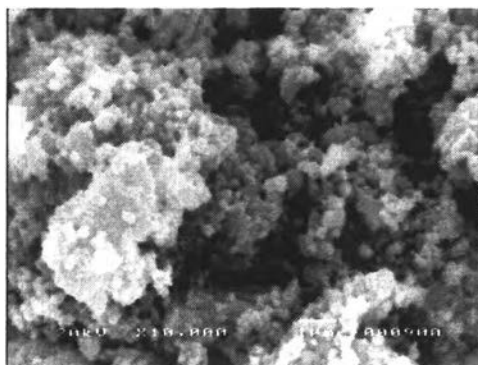
(a) Uncalcined



(d) Calcined at 700 °C



(b) Calcined at 300 °C



(e) Calcined at 900 °C

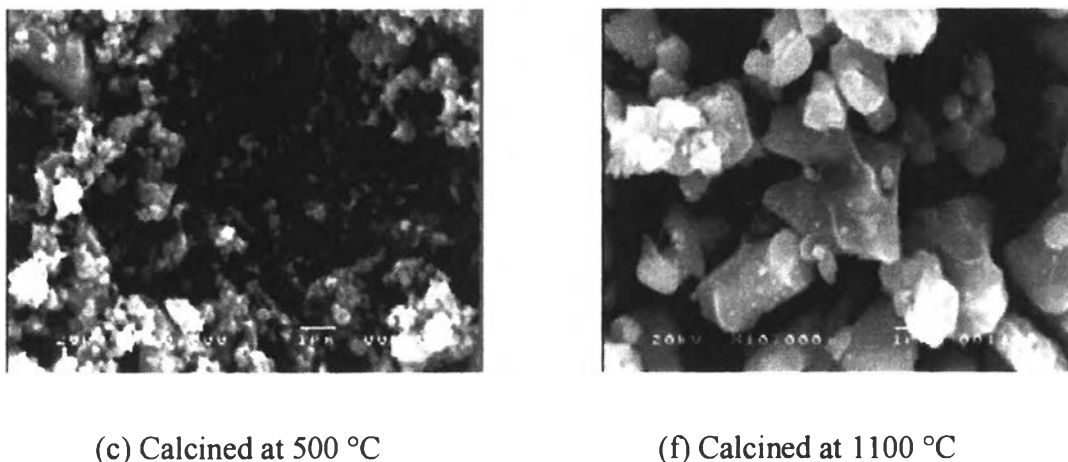


Figure 4.5 SEM micrographs of glycolato titanium calcined at different temperatures, with magnification of 10000.

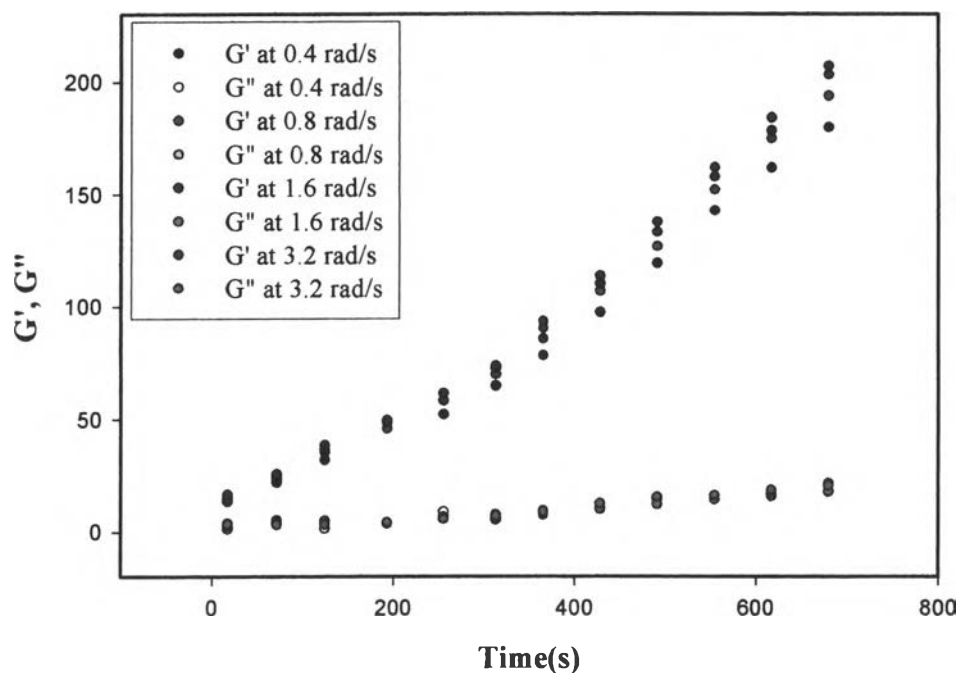
4.2.2 Characterization of Glycolato Titanium Gel

During sol-gel process, the rate of transformation reactions and gelation times were studied using fluid rheometer as described following.

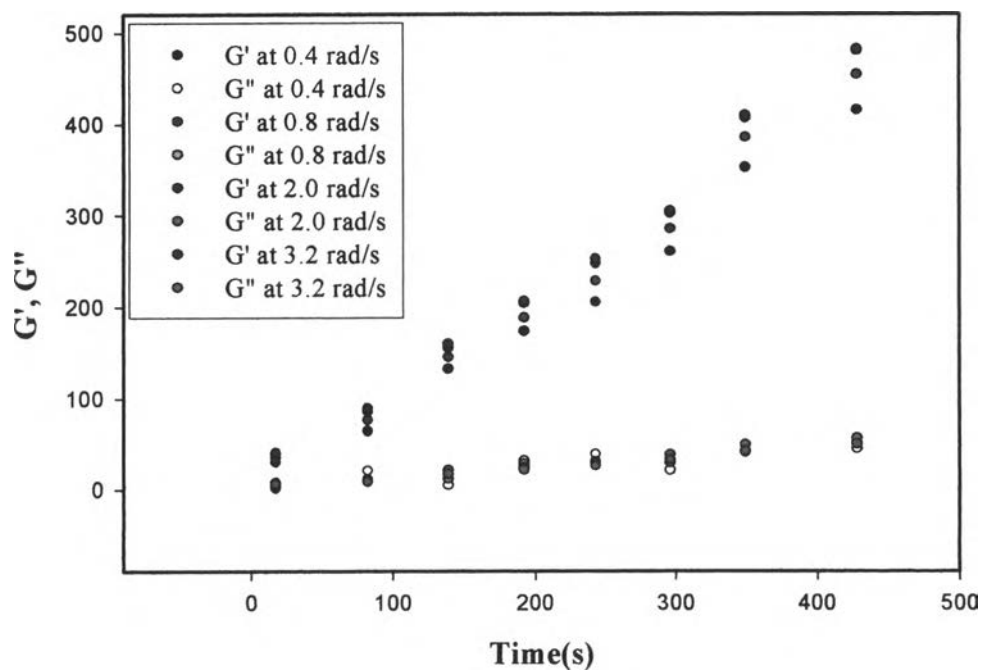
4.2.2.1 *Rheometric Measurement*

Viscoelastic studies of gelation kinetics at various hydrochloric acid and water ratios were carried out by recording the time evolution of the storage moduli (G') and loss moduli (G'') as shown in Figures 4.6a-d. It was used to estimate the gelation kinetic from a measurement of the rate of growth of G' at low deformation frequency. We select the gelation rate as the highest value of the modulus, $G'(\omega = 0.4)$, divided by the elapsed time. Thus, for sample ratio of 35: 125 we obtain $\Delta G'/\Delta t = 0.26$ dynes/cm²sec; for 40: 120, $\Delta G'/\Delta t = 0.99$ dynes/cm²sec; for 45: 115, $\Delta G'/\Delta t = 0.80$ dynes/cm²sec; and for 50: 110, $\Delta G'/\Delta t = 0.44$ dynes/cm²sec. From Figures 4.6a-d also show that the storage modulus (G') increases rapidly whereas the loss modulus (G'') increases more slowly. Thus, even at early stages of hydrolysis, the G' values are much larger than G'' , i.e. the solutions are predominantly elastic in behavior. In case of highest acidity (50: 110), there appears to be a 200 s lag time, where G' and G'' increase little, suggesting that cluster growth

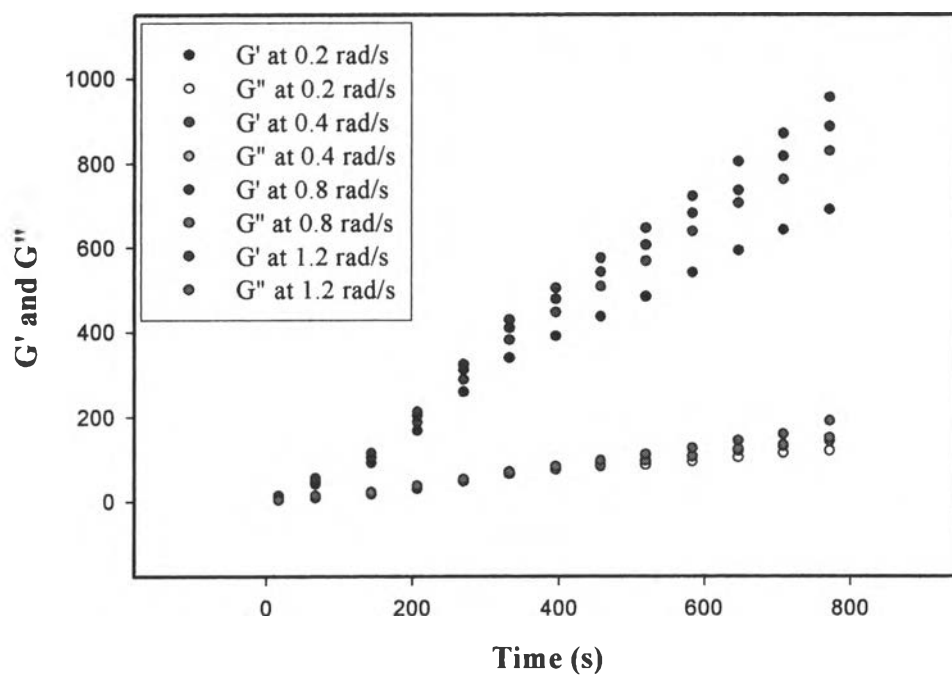
and the network formation initially occur very slowly, but then increase more rapidly after 200 s. This suggests that larger amounts of acid not only hydrolyze but also strongly inhibit the condensation process, thus the network cannot form easily.



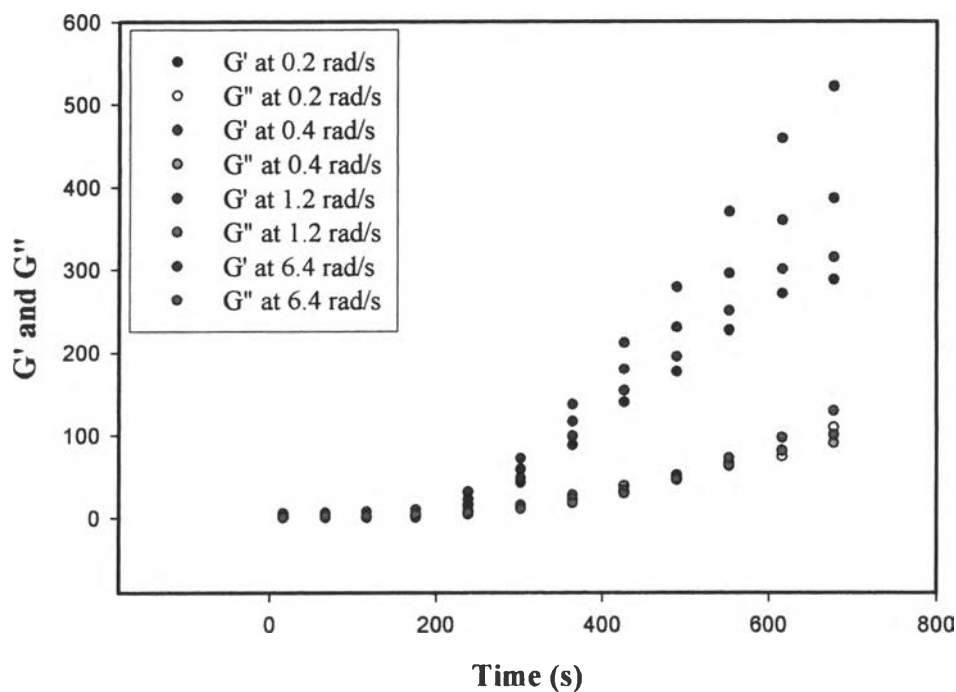
(a) Glycolato titanium gel at ratio 35: 125



(b) Glycolato titanium gel at ratio 40: 120



(c) Glycolato titanium gel at ratio 45: 115

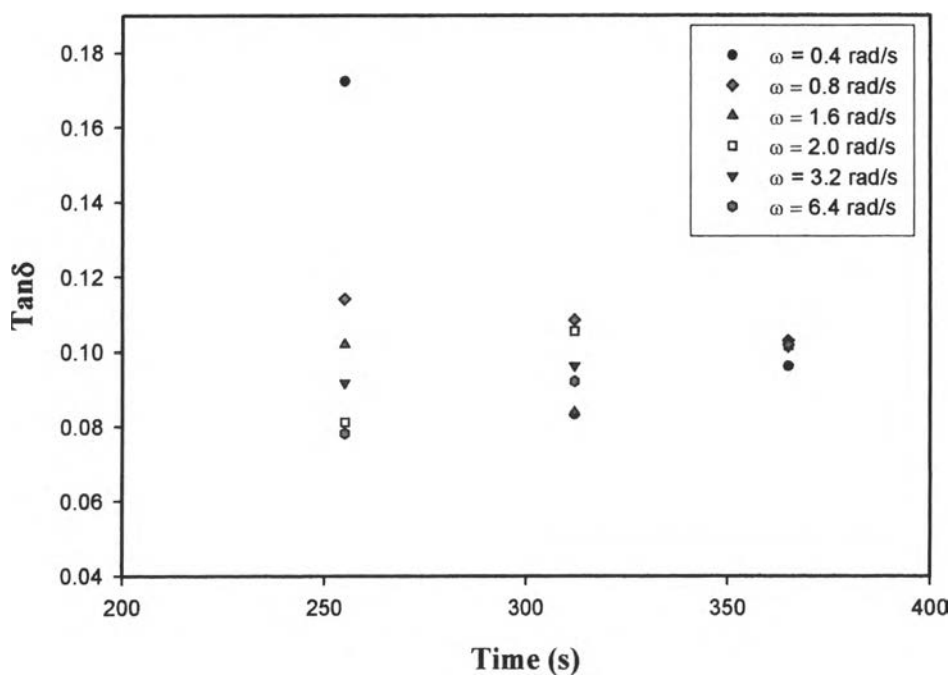


(d) Glycolato titanium gel at ratio 50: 110

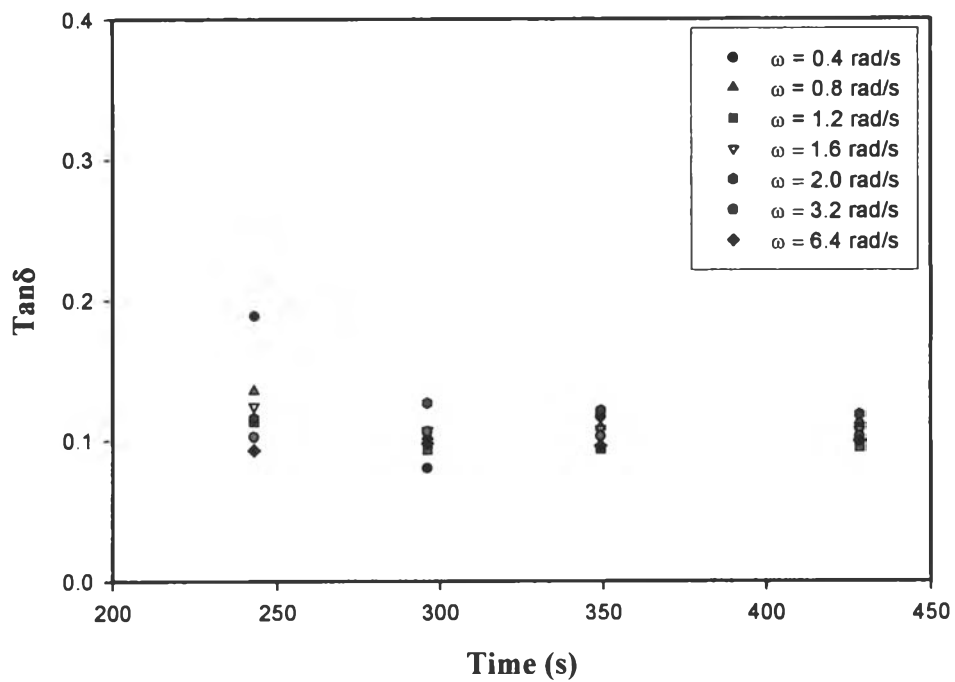
Figure 4.6 The frequency scan of G' and G'' of glycolato titanium gel at different hydrochloric acid and water ratios: a) 35: 125, b) 40: 120, c) 45: 115 and d) 50: 110.

The gelation times can be determined from the crossovers of the graphs of $\tan \delta$ at different frequencies, as shown in Figures 4.7a-d. The gelation time of glycolato titanium gel at the ratio 35: 125, 40: 120, 45: 115 and 50: 110 are 370, 430, 650 and 870 sec, respectively. By comparing the effect of the amount of hydrochloric acid and water ratios, glycolato titanium gel at 35:125 gives the shortest gelation time and the gelation time continues to increase with the increasing hydrochloric acid and water ratios. From this work, it is found the same result to (Ward *et al.*, 1993) work. That is the addition of acid not only hydrolyzes the product but also increases the gelation times by decreasing the rate of condensation. Qualitatively, the condensation rate is inversely proportional to gelation time. With the addition of enough acid, condensation can be prevented entirely (Livage *et al.*, 1988). This can be explained by the protonation of the hydroxo ligands. The hydroxo ligands of the metal atom are protonated to form

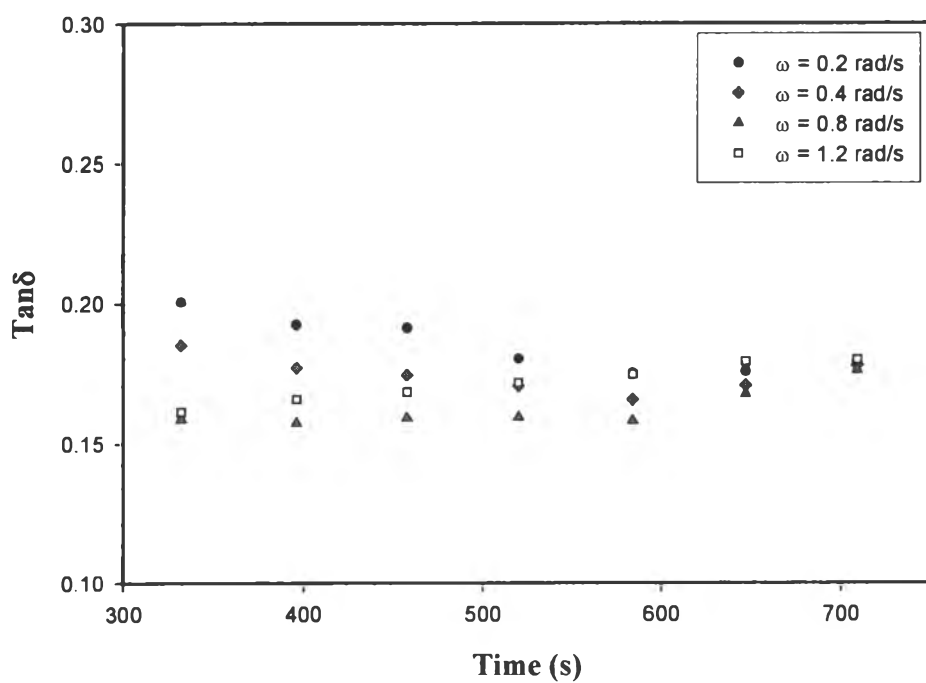
M-OH₂⁺. The oxygen atom is no longer nucleophilic, decreasing the driving force for substitution. As more acid is added to the system, more hydroxo ligands are protonated and the condensation reactions slows, increasing the gelation time as stated by (Ward *et al.*, 1993).



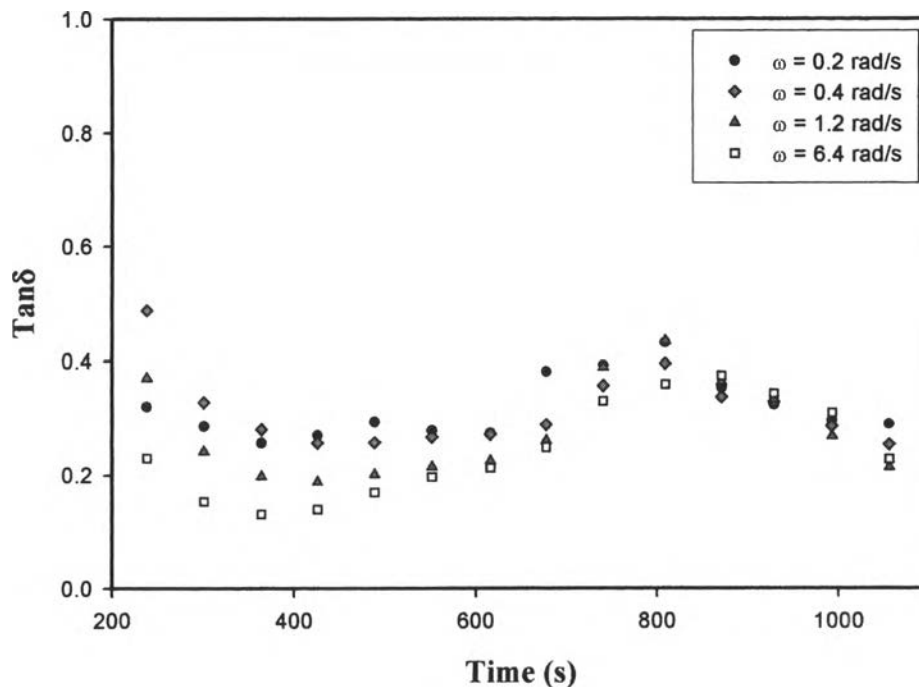
(a) Glycolato titanium gel at ratio 35: 125



(b) Glycolato titanium gel at ratio 40: 120



(c) Glycolato titanium gel at ratio 45: 115



(d) Glycolato titanium gel at ratio 50: 110

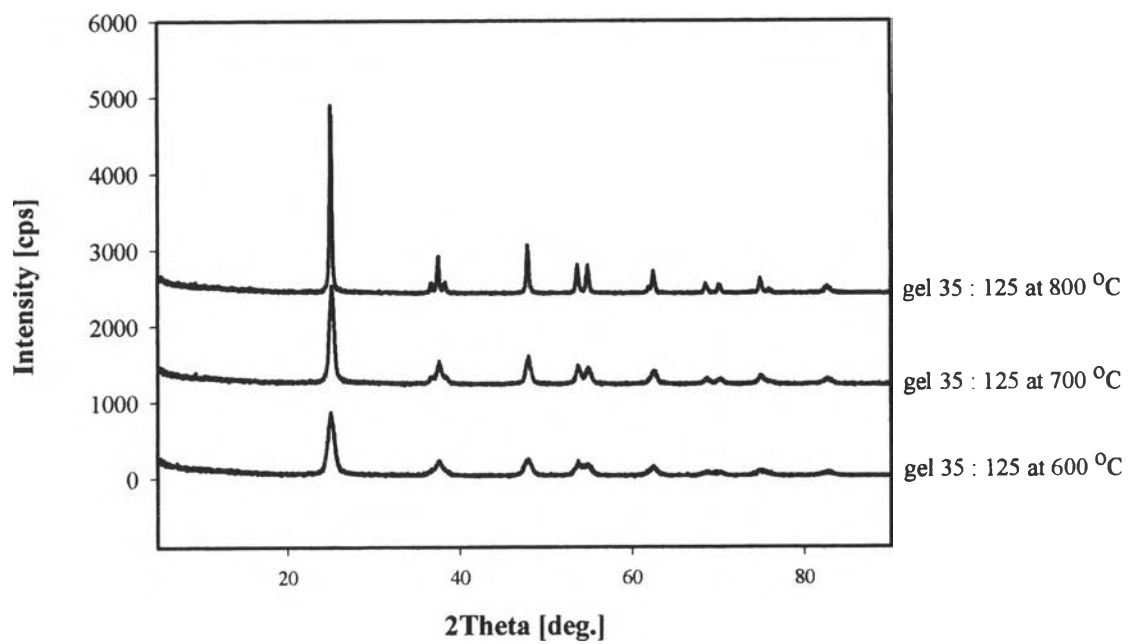
Figure 4.7 The frequency scan of $\tan\delta$ of glycolato titanium gel at different hydrochloric acid and water ratios: a) 35: 125, b) 40: 120, c) 45: 115 and d) 50: 110.

4.2.3 Characterization of Titania Powder

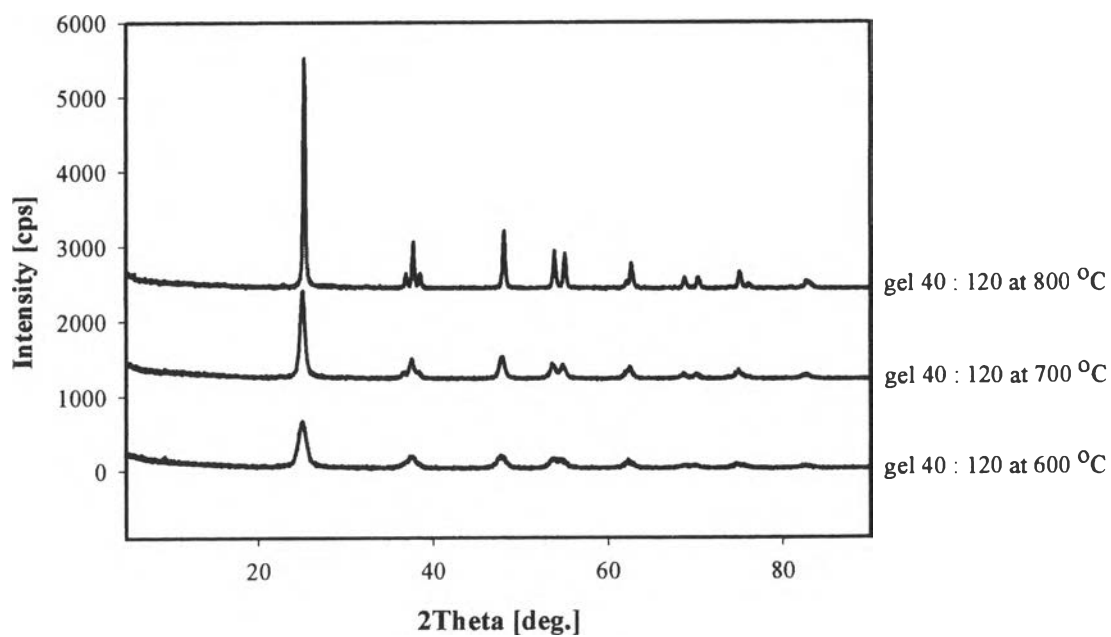
The obtained titania powder after passed through the sol-gel process was identified using XRD and SEM. The surface area was also measured using BET as described below.

4.2.3.1 *X-Ray Diffraction (XRD)*

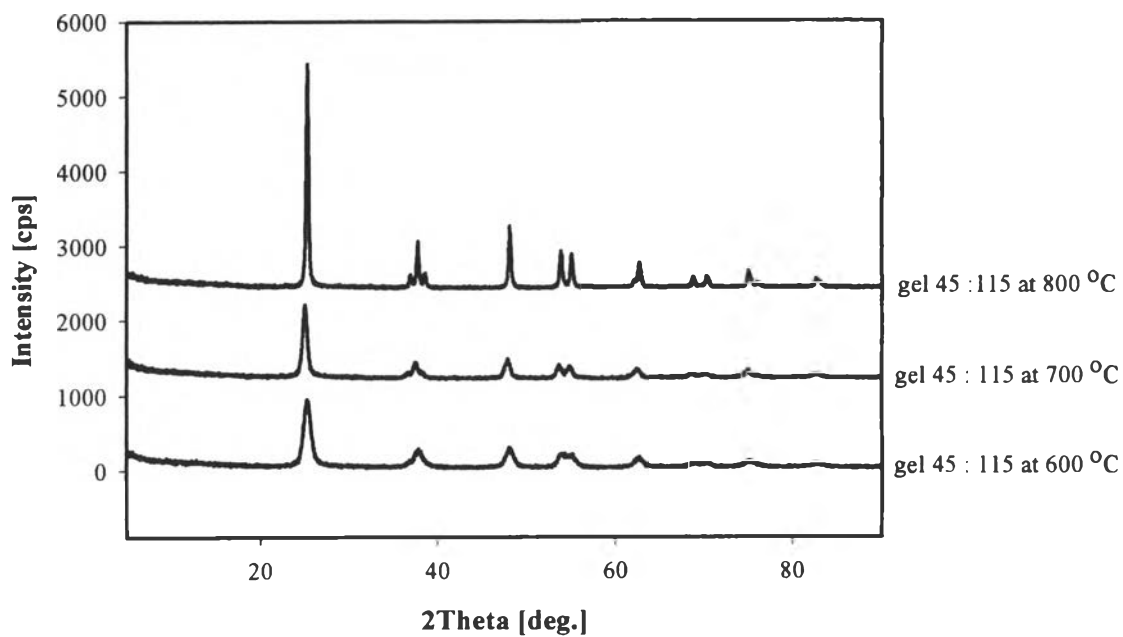
The XRD patterns were used to identify the obtained titania powder at different hydrochloric acid and water ratios, as shown in Figures 4.8a-d. Titania powder at different calcination temperatures between 600° to 800 °C can be identified as the anatase form. The crystallinity of the obtained titania increases with increasing calcination temperature.



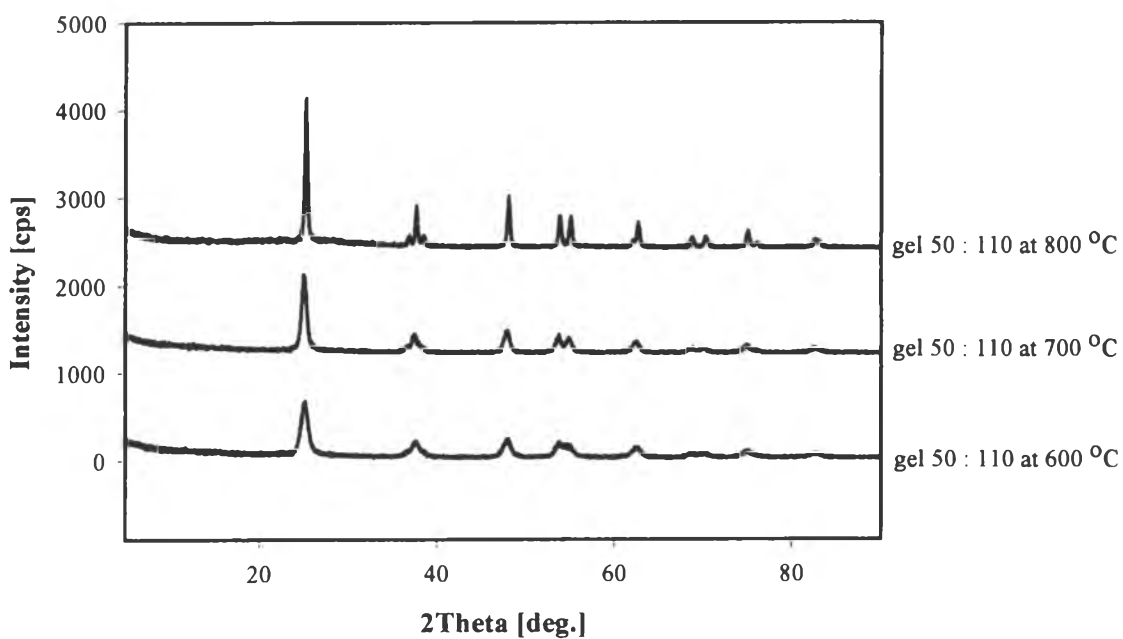
(a) Titania powder at ratio 35: 125



(b) Titania powder at ratio 40: 120



(c) Titania powder at ratio 45: 115

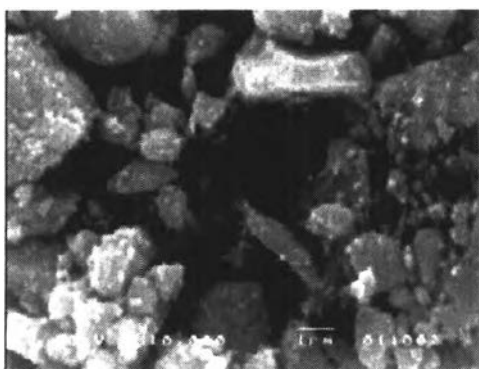


(d) Titania powder at ratio 50: 110

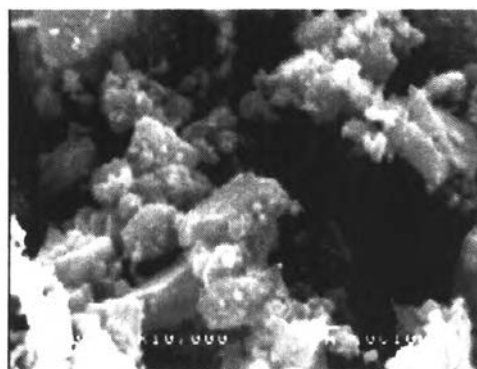
Figure 4.8 XRD patterns of titania powder calcined at different temperatures and different hydrochloric acid and water ratios: a) 35: 125, b) 40: 120, c) 45: 115 and d) 50: 110.

4.2.3.2 Scanning Electron Microscopy (SEM)

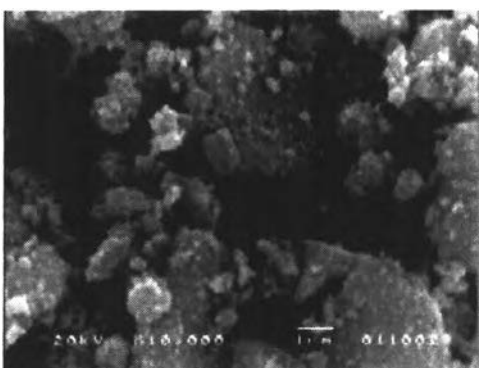
The SEM micrographs of the obtained titania powder at different hydrochloric acid and water ratios are shown in Figures 4.9a-l. At lower temperature, the larger particles of anatase titania are formed due to lower crystallinity. Upon calcinations at 800 °C, the anatase titania was completely obtained (supported by the XRD results in Figure 4.8). As compared between hydrochloric acid and water ratios, the lower particles will be obtained at smaller acid and water ratios.



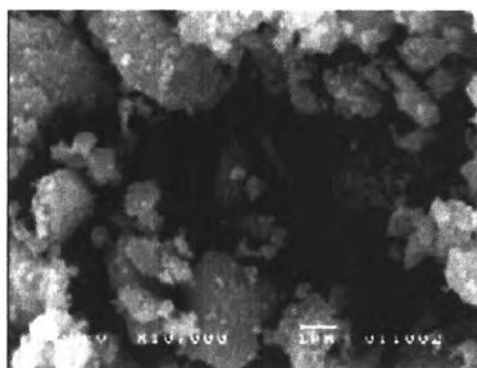
(a) Titania powder 35: 125, 600 °C



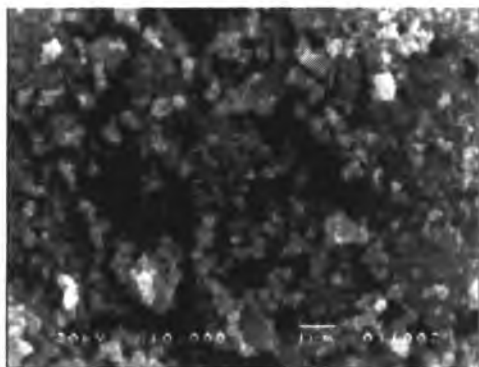
(d) Titania powder 40: 120, 600 °C



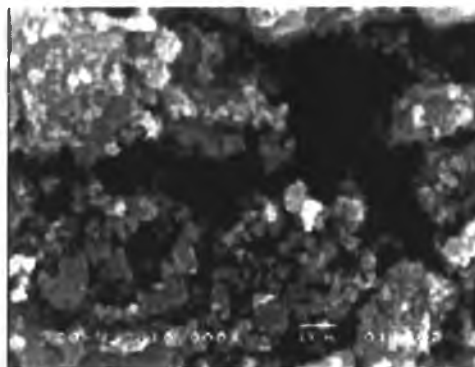
(b) Titania powder 35: 125, 700 °C



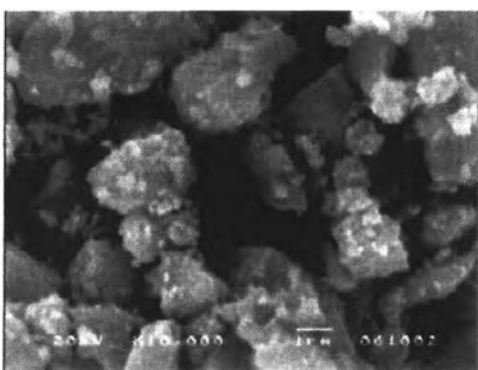
(e) Titania powder 40: 120, 700 °C



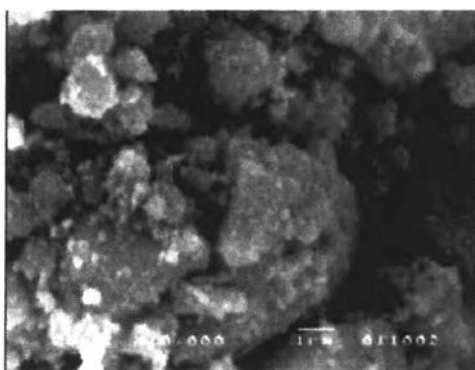
(c) Titania powder 35: 125, 800 °C



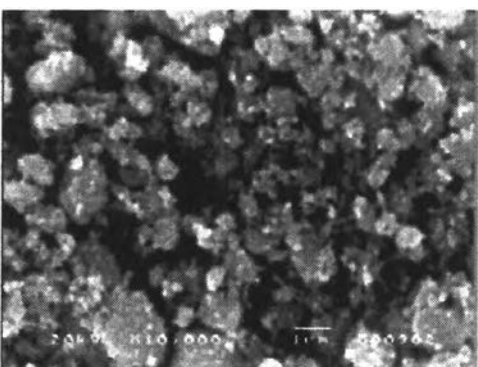
(f) Titania powder 40: 120, 800 °C



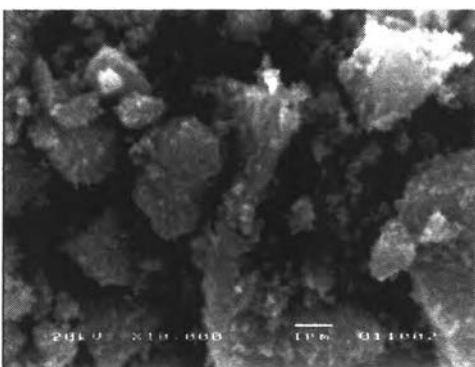
(g) Titania powder 45: 115, 600 °C



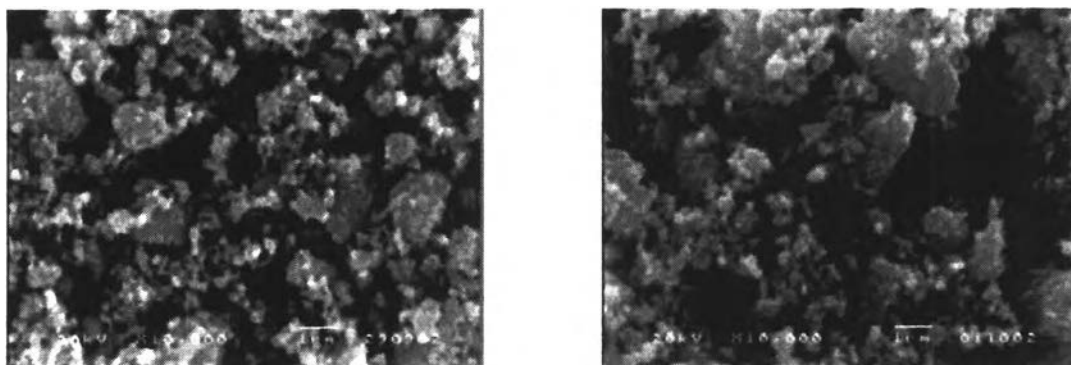
(j) Titania powder 50:110, 600 °C



(h) Titania powder 45: 115, 700 °C



(k) Titania powder 50:110, 700 °C



(i) Titania powder 45: 115, 800 °C

(l) Titania powder 50: 110, 800 °C

Figure 4.9 SEM micrographs of titania powder calcined at different temperatures and different hydrochloric acid and water ratios: a-c) 35: 125, 600° to 800 °C, d-f) 40: 120, 600° to 800 °C, g-i) 45: 115, 600° to 800 °C, j-l) 50: 110, 600° to 800 °C.

4.2.3.3 BET Surface Area Measurement

In this section, the effect of various hydrochloric acid and water ratios and calcination temperatures on the product surface area are studied by BET technique and the surface area of titania powder is summarized in Table 4.4.

Table 4.4 Surface area of titania powder obtained from various hydrochloric acid and water ratios at different calcined temperatures

Temperature (°C)	Surface area (m ² /g)			
	35: 125	40: 120	45: 115	50: 110
600	125	111	107	105
700	60	59	55	50
800	20	18	17	15

The highest surface area, 125 m²/g, is obtained from titania at the lowest acid and water ratio of 35:125 and calcined at 600 °C. With increasing hydrochloric acid and water ratios, the surface area of the products are decreased dramatically. Furthermore, the surface area of titania powder can be related to

gelation times. At lower acid and water ratios (lower gelation times), the condensation reactions are slowed down so that more bridging could occur between small growing particles. The resulting gel network has a larger surface area. As the gelation times lengthened further (higher acid and water ratios), the condensation reactions are slowed down so much that the large particles are formed with the little bridging between them. This network contains large particles, and hence the surface area is decreased (Ward *et al.*, 1993). Upon calcinations at higher temperatures, the surface area are also decreased rapidly because the occurrence of agglomeration as stated by (Kim, 2001). As compare the surface area of as-prepared titania to the titania powder obtained from the hydrolysis of TiCl_4 (Zhang *et al.*, 2000) at various calcination temperatures. The as-prepared titania powder has higher surface area than those technique. Therefore, the as-prepared titania powder is suitable for preparing of high surface area anatase titania.